

Direct Simulation of Rotational Relaxation Using State-to-State Cross Sections

Darrin L. Willauer* and Philip L. Varghese†
University of Texas at Austin, Austin, Texas 78712

Rotational relaxation in para-hydrogen ($p\text{-H}_2$) is modeled using a direct simulation Monte Carlo (DSMC) method with state-to-state collision cross sections and the results are compared with a simple Borgnakke-Larsen (B-L) type rotational relaxation model. The detailed simulation shows that the rotational population relaxes through nonBoltzmann distributions as expected. However, even the rotational energy relaxation shows some unexpected features that cannot be described by the simple model. For initial states with strong nonequilibrium, the simple B-L model fails to provide even a qualitative description of the relaxation of the rotational energy of $p\text{-H}_2$.

Introduction

THE most common method used to solve rarefied flow fields is the direct simulation Monte Carlo (DSMC) method pioneered by Bird.¹ The DSMC method involves simulating the flow physics as opposed to solving the conservation equations for mass, momentum, and energy. The flow is modeled on the molecular level using a relatively small number of simulated molecules. Although it has not yet been proven that the DSMC method is guaranteed to converge to a solution of the Boltzmann equation, it is very widely used because of its efficiency and simplicity.

There is considerable interest in developing accurate models for rotational and vibrational energy relaxation because of the influence that nonequilibrium populations can have on the chemical reactivity of the gas. For example, dissociation occurs predominantly from highly excited vibrational states.² Rotational energy also affects the chemical reaction rate by reducing the number of bound vibrational states in a rapidly rotating molecule.³

Most current DSMC calculations use a simple variable hard sphere (VHS) model for the elastic collision cross section.⁴ Although this is a powerful and useful simplification, the "best" power law exponent to be used in simulations tends to depend on the flow conditions. Intermolecular energy exchange is usually simulated by means of a derivative of the Borgnakke-Larsen (B-L) model⁵ with vibration and rotation collision numbers used to specify the rate of vibrational and rotational relaxation relative to the elastic collision frequency. Rotational relaxation is often assumed to be fast with a rotational collision number $Z_R = 5$. Models for temperature-dependent rotational collision numbers have been proposed in Refs. 6–8. Boyd⁹ has given a form for the probability of rotational energy transfer that reproduces the Parker⁶ result when using the VHS model in a DSMC computation. These models treat the internal energy as a continuous variable. It is also assumed that one only needs to track the rotational temperature, defined in terms of the mean rotational energy of the distribution. This involves an implicit assumption that the rotational population is at least approximately Boltzmann distributed. However, it is well known that rotational distributions

do not relax to equilibrium through intermediate Boltzmann distributions.¹⁰ This article is part of an effort to simulate internal state relaxation more accurately in DSMC calculations and to assess the complexity and computational cost of the more accurate procedure.

We have performed DSMC calculations of spatially homogeneous rotational relaxation of para-hydrogen ($p\text{-H}_2$), tracking individual quantum rotational states, and using state-to-state collision cross sections to compute the rates of intermolecular energy transfer. The results of the calculations are compared to those obtained using a B-L-type model. We chose to study rotational relaxation of $p\text{-H}_2$ for several reasons. Most importantly, the master equation calculations of Rabitz and Lam¹⁰ provide a benchmark to check the accuracy of our calculations. The rotational levels of $p\text{-H}_2$ are widely spaced so the effects of quantization are significant at ordinary temperatures and only a few excited rotational states are populated. This made the preliminary modeling manageable. Because the vibrational energy level spacing is large, the vibrational energy is effectively "frozen" and does not need to be considered. Finally, there is a reasonable data base on the state-to-state cross sections for hydrogen so that the detailed calculations are based on realistic numbers. Although the simulation was run for $p\text{-H}_2$, the methodology is general and can be applied to any gas, provided one has reasonable estimates for the state-to-state cross sections.

Modeling

Collision Cross Sections

We have used rotational state-to-state collision cross sections calculated by Zarur and Rabitz.¹¹ They present extensive results calculated from the "effective potential" method which are in close accord with the more rigorous close-coupling calculations of Green¹² and Monchick and Schaefer.¹³ Zarur and Rabitz calculated elastic and excitation collision cross sections for individual processes $J_i J_j \rightarrow J_i' J_j'$, where J_i denotes the rotational quantum number of state i . Cross sections were presented in tabular form as a function of the total energy of the colliding pair ϵ_i . The cross sections were transformed to functions of the relative kinetic energy ϵ_{ir} by subtracting the energy contained in rotational levels J_i and J_j from the total energy of the colliding pair

$$\epsilon_{ir} = \epsilon_i - (\epsilon_{ri} + \epsilon_{rj}) \quad (1)$$

Using the rigid rotor approximation, the energy of a particular rotational level with quantum number J is given by

$$\epsilon_r(J) = J(J + 1)k\theta, \quad (2a)$$

Presented as Paper 91-1342 at the AIAA 26th Thermophysics Conference, Honolulu, HI, June 24–26, 1991; received Aug. 9, 1991; revision received Dec. 19, 1991; accepted for publication Dec. 19, 1991. Copyright © 1991 by the American Institute of Aeronautics and Astronautics, Inc. All rights reserved.

*Graduate Student, Department of Mechanical Engineering.

†Associate Professor, Department of Aerospace Engineering and Engineering Mechanics. Senior Member AIAA.

$$= J(J + 1)hcB \quad (2b)$$

Here k is Boltzmann's const, θ_r is the characteristic rotational temperature, h is Planck's const, c is the velocity of light, and $B[\text{cm}^{-1}]$ is the spectroscopic rotational const (B_v or B_0 , see below). Once the data were transformed, the elastic collision cross sections were curve-fit with power law equations while the excitation collision cross sections were curve-fit with third order polynomials. These equations were kept simple to reduce computational time and cost because a new collision cross section must be calculated each time a collision pair is sampled.

Zarur and Rabitz only provide the elastic and excitation collision cross sections, so the de-excitation cross sections were calculated using the principle of detailed balance. For identical particles the de-excitation collision cross section $\sigma_{i'j' \rightarrow ij}$ at ϵ_{ir} is related to the excitation collision cross section $\sigma_{ij \rightarrow i'j'}$ at ϵ_{ir} by

$$\sigma_{i'j' \rightarrow ij}(\epsilon_{ir}) = \frac{(1 + \delta_{ij})(2i' + 1)(2j' + 1)}{(1 + \delta_{i'j'})(2i + 1)(2j + 1)} \frac{\epsilon_{ir}'}{\epsilon_{ir}} \sigma_{ij \rightarrow i'j'}(\epsilon_{ir}') \quad (3)$$

where

$$\epsilon_{ir}' = \epsilon_{ir} + \Delta\epsilon \quad (4a)$$

$$\Delta\epsilon = (\epsilon_{ri} + \epsilon_{rj}) - (\epsilon_{ri'} + \epsilon_{rj'}) \approx 0 \quad (4b)$$

Here $\Delta\epsilon$ is the net increase in rotational energy during the excitation process, and the kinetic energies for excitation and de-excitation processes are related by conservation of energy. The Kronecker deltas account for symmetry factors in the definitions of the cross sections used in Ref. 11, and arise when either the initial or final quantum states of the molecules are identical. When using ordered pairs to describe the process ($ij \rightarrow i'j'$), two processes must be accounted for in general, the "direct" process ($i \rightarrow i', j \rightarrow j'$) and the "exchange" process ($i \rightarrow j', j \rightarrow i'$). However, when either the final or initial states are identical, the direct and exchange processes are the same and the factor of symmetry is needed to prevent double counting.

To guarantee detailed balance, de-excitation cross sections were always calculated using Eq. (3) with the corresponding excitation cross section determined from the curve-fits. We tried to use curve-fits to de-excitation cross sections calculated from Eq. (3), but found they did not maintain detailed balancing over many collisions. This is because the curves satisfied detailed balance exactly at the fitting points, but not between them.

Collision Pair Sampling

Collisions were sampled using a modified version of the "no-time-counter" method¹⁴ to determine the rates of individual elastic and inelastic processes. Each rotational level is treated as a separate species. Because we simulated $p\text{-H}_2$, only the even rotational quantum numbers were needed. (Ortho- (o -) and para- (p -) states of H_2 arise from nuclear spin; o -states are symmetric and p -states are antisymmetric with respect to exchange of the nuclei. Because H nuclei are fermions, the overall molecular state must be antisymmetric with respect to nuclear exchange. Thus, p -states only occur with even rotational quantum number J , whereas o -states only occur with odd J . This simplifies the modeling problem because processes that mix nuclear spin states are very unlikely.)

The rotational level of each molecule is stored in a cross-referencing array similar to that used for determining the spatial location of the molecules. This allows efficient sampling of molecules from a particular species (rotational state). The number of random pair selections $\eta_{ij \rightarrow i'j'}$ for a collision process specified by the ordered pairs $(J_i, J_j) \rightarrow (J_{i'}, J_{j'})$ is calculated from

$$\eta_{ij \rightarrow i'j'} = [1/(1 + \delta_{ij})] N n r_i r_j \Delta t (\sigma_{ij \rightarrow i'j'} v_r)_{\max} \quad (5)$$

where N is the number of simulated molecules, n is the number density of the gas, r_i is the fraction of molecules in a particular state i , $(\sigma_{ij \rightarrow i'j'} v_r)_{\max}$ is the maximum product of the relative velocity v_r and the state-to-state collision cross section, and Δt is the global time step. Ordered pairs are defined by $j \geq i, j' \geq i'$.¹¹ The Kronecker delta function is used to generate the symmetry factor when $j = i$. Equation (5) is very similar to one derived by Baganoff and McDonald.¹⁵ The difference is that Eq. (5) is applied to individual processes of individual species, whereas Eq. (20) of Ref. 15 was applied only to collisions between individual species. Equation (5) is the general form of the no-time-counter method and can be shown to reproduce the standard no-time-counter method when $i = j = i' = j'$.

$$\eta = \frac{1}{2} N n (1)^2 \Delta t (\sigma v_r)_{\max} \quad (6)$$

Knowing the number of samples η for each process ($ij \rightarrow i'j'$), random pairs of molecules in the specified initial states are selected and the product of their relative velocity and collision cross-section is calculated. A random number is drawn and compared to the value of $(v_r \sigma_{ij \rightarrow i'j'}) / (v_r \sigma_{ij \rightarrow i'j'})_{\max}$. The pair is accepted if the random number is smaller than the ratio, otherwise a new random pair is chosen. Excitation processes are automatically forbidden when the relative kinetic energy of the selected pair is less than the excitation energy, because the cross-sections are explicit functions of the relative kinetic energy. If the pair is selected for collision by the acceptance-rejection procedure, the rotational energy is distributed according to the rotational levels specified by the transition. The magnitude of the postcollision relative velocity vector is determined by the conservation of energy, and its orientation is randomly chosen from a spherically symmetric distribution. This procedure is repeated for each collision process. Note that elastic processes are treated in the same way as inelastic processes, and correspond to the special case $ij \rightarrow ij$.

The ratio r_i is updated at the beginning of each global time step. Our method is equivalent to a standard no-time-counter method, therefore the computation time is proportional to the number of simulated molecules. The number of collision pairs sampled for particular processes (typically involving high J states) can be quite small compared to other processes which result in large statistical fluctuations in the populations of these states. This was remedied by artificially increasing the maximum product, $(v_r \sigma_{ij \rightarrow i'j'})_{\max}$, by a factor β , to give more samples for these processes. This factor was then included in the acceptance-rejection process. Note that β is not the same as the typical species or regional weighting factors because it is a function of the particular collision process and does not affect the density. It is used to ensure that a statistically meaningful number of collision pairs are sampled relative to the other collision processes.

Temperature Definition

Mode temperatures (translational, rotational, vibrational) can be meaningfully defined in a nonequilibrium situation, provided the modes are Boltzmann distributed. In this context the temperatures can be regarded as the parameters that describe the population distributions over the quantized energy states of the corresponding mode. Relaxation proceeds by means of a series of intermediate population distributions that are non-Boltzmann, because the quantized rotational states are not equally spaced. Although one can still define a rotational temperature based on the mean rotational energy, this parameter must be treated with caution. Two non-Boltzmann distributions having the same mean energy, and thus the same rotational temperature, may behave very differently. For example, their chemical reactivity and relaxation rates might differ significantly.

The quantized rotational distributions of H_2 were calculated for a characteristic rotational temperature $\theta_r = 87.65$ K. This

value was calculated [cf. Eqs. (2a) and (2b)] from the spectroscopic rotational constant B_e which corresponds to the equilibrium internuclear separation.¹⁶ This procedure is consistent with a rigid-rotor model, but it might have been preferable to use the rotational constant of the vibrational ground state B_0 to simulate hydrogen most accurately; this would give $\theta_r = 85.4$ K. (The decrease in θ_r arises from the slight increase in the effective moment of inertia due to the zero-point vibration of the H_2 molecule in its ground state.) However, a sample calculation showed that the slight change in θ_r did not affect the results appreciably.

We use rotational temperature because it is so commonly reported in the literature. We define the rotational temperature T_r of a nonequilibrium distribution to be the temperature of a quantized Boltzmann distribution that has the same mean energy as the given distribution. The DSMC simulations in this work had J restricted to 0, 2, 4, or 6; the mean energy of an arbitrary truncated distribution is given by

$$\varepsilon_{r,m} = \sum_{i=0}^{i_{\max}} 2i(2i+1)k\theta_r(n_{2i}/n_t) \quad (7)$$

where n_{2i}/n_t is the fractional population in level $2i$. The corresponding relation for a Boltzmann distribution is explicitly

$$\varepsilon_{r,m}^*(T_r) = \frac{1}{Q_r(T_r)} \sum_{J=0,2,\dots} J(J+1)k\theta_r(2J+1) \cdot \exp \left[-\frac{J(J+1)\theta_r}{T_r} \right] \quad (8)$$

where the rotational partition function is

$$Q_r(T_r) = \sum_{J=0,2,\dots} (2J+1) \exp \left[-\frac{J(J+1)\theta_r}{T_r} \right] \quad (9)$$

The sums over J in Eqs. (8) and (9) are taken over all even J values that contributed at the specified T_r , i.e., these sums are not truncated at $J = 6$. Nuclear spin degeneracy has been neglected in Eqs. (7–9) because the sums are taken over a single spin modification (para in our case). Figure 1 shows the mean rotational energy of Boltzmann distributed $p\text{-}H_2$ as a function of rotational temperature. This curve was used to determine the rotational temperature of arbitrary distributions with specified mean rotational energy. Figure 1 also shows the classical (nonquantized) equipartition relation between mean energy and rotational temperature of a diatomic

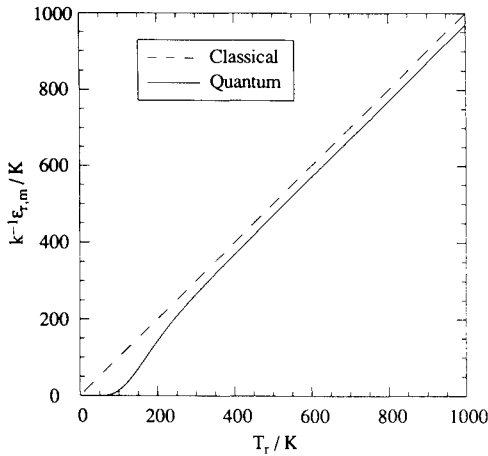


Fig. 1 Mean rotational energy of $p\text{-}H_2$ at equilibrium as a function of rotational temperature. The energy is divided by Boltzmann's constant to give units of Kelvins. A characteristic rotational temperature $\theta_r = 87.65$ K was used for the quantum calculation. This curve is used to define rotational temperature in a nonequilibrium gas. The classical value is shown for comparison.

molecule. Note that there is a significant difference between the two curves over a substantial temperature range.

Results and Discussion

We have validated the code by repeating some of the calculations of Rabitz and Lam¹⁰ who studied rotational relaxation of $p\text{-}H_2$ using a master equation formulation. Our procedure is somewhat more general because the DSMC method does not require the assumption that the velocity distribution remains Maxwellian. Simultaneous translational and rotational relaxation can be modeled using our technique. However, the assumption of a Maxwellian velocity distribution is quite good for hydrogen because rotational relaxation is very slow. Therefore, our results can be compared directly with those of Ref. 10; the agreement with the master equation results is very good. We present some representative results and the following discussion is focused on the implications of the results for DSMC simulations. The discussion is couched in terms of nearest-neighbor transitions. Multiple quantum transitions are included in the modeling, but the cross sections are much smaller, and nearest-neighbor transitions ($\Delta J = \pm 2$) tend to dominate.

We calculated the spatially homogeneous relaxation of $p\text{-}H_2$ starting from a Maxwellian velocity distribution at 300 K and a Boltzmann rotational distribution at 700 K. More than 99.9% of the $p\text{-}H_2$ molecules have $J \leq 6$ at 700 K, so little error is introduced by truncating the rotational distribution in the DSMC simulation. The results were obtained by averaging three simulations of 1000 molecules each. The computational time step t_c of 1.25 ns is about one-fifth the mean time between collisions τ_c calculated at the initial translational temperature (300 K) using a hard-sphere collision diameter of 0.293 nm.¹¹

Figure 2 shows the evolution of the individual state populations with time. The relaxation proceeds initially with a relatively rapid equilibration of state 0 within about $300\tau_c$ ($t_c = 1500$), by a transfer of population from state 2. The equilibration of states 2 and 4 is slower and results in a net repopulation of state 2. The relaxation of state 6 is the slowest, and the equilibration with state 4 results in a slight net increase in state 4 population as it approaches the final equilibrium. It is clear from the plot that the relaxation is quite complex, with populations of states 0 and 6 showing monotonic relaxation, while states 2 and 4 show minima (the former being much more pronounced than the latter).

The relaxation of the rotational energy plotted in Fig. 3 shows none of these complexities. The mean rotational energy and the corresponding rotational temperature approach equilibrium in approximately $2600\tau_c$, i.e., $t_c \approx 13,000$. Careful inspection of Fig. 2 shows that state 6 has not completely equilibrated at this time and requires about $7000\tau_c$ ($t_c \approx 35,000$)

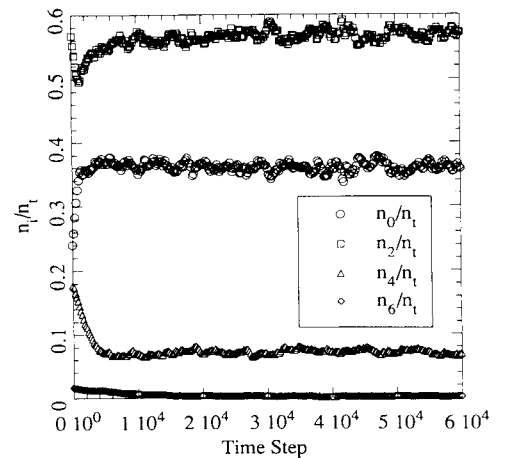


Fig. 2 Fractional populations in individual rotational states during relaxation of $p\text{-}H_2$ initially at $T_r = 300$ K (Maxwellian) and $T_r = 700$ K (Boltzmann). The computational time step is 1.25 ns.

before reaching equilibrium. This has little effect on the mean rotational energy because the equilibrium population in this state is very small at this temperature (456 K). Figure 3 also shows the results obtained using a standard Borgnakke-Larsen relaxation with a constant rotational collision number $Z_R = 300$. This is approximately the value determined by acoustic measurements and distorted wave calculations near room temperature.¹⁷ It is clear from Fig. 3 that Z_R is too large to simulate the energy relaxation. However, as noted above in the discussion of Fig. 2, $Z_R \approx 300$ describes the equilibration of states 0 and 2 quite well. Independent theoretical calculations of $Z_{R,4 \rightarrow 2}$ give a value of 660 at 300 K.¹⁷ This is also confirmed by the population trends in Fig. 2. The values of Z_R reported in the literature refer to the number of collisions required for population relaxation and do not apply to the collision number for energy relaxation required by B-L models. The value of Z_R required to describe the energy relaxation by the B-L model is less than the smallest value describing the population relaxation (at least for p -H₂). This is surprising and counter to our intuition.

It is possible to obtain better agreement with the state-to-state relaxation model by using a smaller value for Z_R in the B-L model. This is shown in Fig. 4, which gives the results of the relaxation with $Z_R = 100$. The agreement is clearly much better, although there are still systematic deviations at early times. Although this approach can give reasonable re-

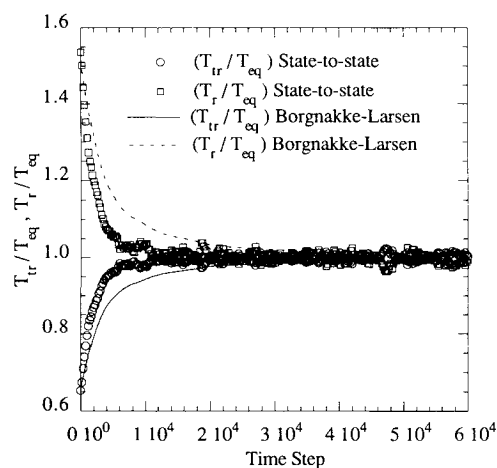


Fig. 3 Translational and rotational temperatures during relaxation of p -H₂ initially at $T_{tr} = 300$ K (Maxwellian) and $T_r = 700$ K (Boltzmann). The calculation with state-to-state collision cross sections is compared to the B-L model with $Z_R = 300$ (const).

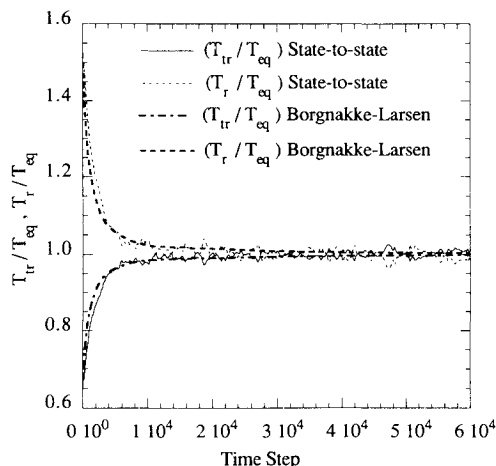


Fig. 4 Translational and rotational temperatures during relaxation of p -H₂ initially at $T_{tr} = 300$ K (Maxwellian) and $T_r = 700$ K (Boltzmann). The calculation with state-to-state collision cross sections is compared to the B-L model with $Z_R = 100$ (const).

sults, the value of Z_R used in the B-L model must be determined by trial and error. Therefore, when using the B-L model, the value of Z_R given in the literature should be checked to ensure it is valid for energy relaxation and not population relaxation as typically given.

Unfortunately, this approach is not guaranteed to work in all cases. We examine the relaxation of three rotational distributions with an initial mean rotational energy of 0.10 eV ($T_r = 1190$ K) and a Maxwellian translational distribution with mean kinetic energy of 0.05 eV ($T_{tr} = 390$ K). The rotational distributions for each case (I–III) are summarized in the table in Fig. 5 which shows the relaxation of the mean rotational energy (expressed in terms of T_r) for each case. The results are plotted against tp instead of t to provide a direct comparison with the results in Ref. 10. Although each case has the same final equilibrium state (as expected), the approach to equilibrium is quite different. Figures 6–8 show the calculated populations of the rotational states as a function of time for each case. Although it might appear that cases I and II could be modeled by a suitably adjusted B-L model, the relaxation is actually quite complex. Figure 9 shows the temporal evolution of T_{tr} and T_r for case I. There is evidence that the rotational temperature drops below the translational temperature and then rises slowly to the final equilibrium value. This overshoot occurs because of the more rapid equi-

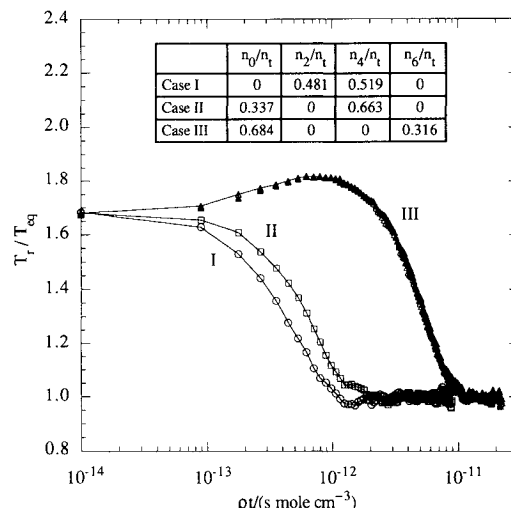


Fig. 5 Variation of rotational temperature with time during relaxation of p -H₂ for three different rotational distributions with the same initial mean rotational energy 0.1 eV ($T_r = 1190$ K). The initial translational distribution is Maxwellian with mean kinetic energy 0.05 eV ($T_{tr} = 390$ K).

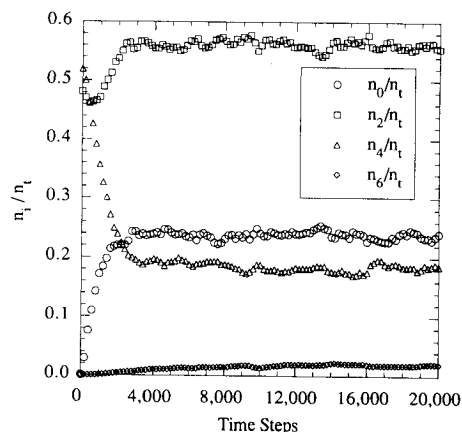


Fig. 6 Fractional populations in individual rotational states during relaxation of case I of Fig. 5. Initial population fractions: $n_0/n_t = 0$, $n_2/n_t = 0.481$, $n_4/n_t = 0.519$, and $n_6/n_t = 0$. The computational time step is 1.43 ns.

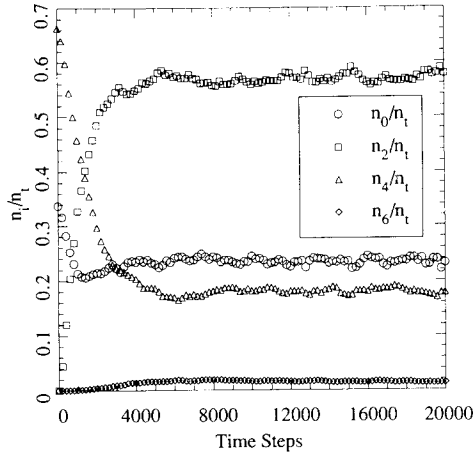


Fig. 7 Fractional populations in individual rotational states during relaxation of case II of Fig. 5. Initial population fractions: $n_0/n_1 = 0.337$, $n_2/n_1 = 0$, $n_4/n_1 = 0.663$, and $n_6/n_1 = 0$.

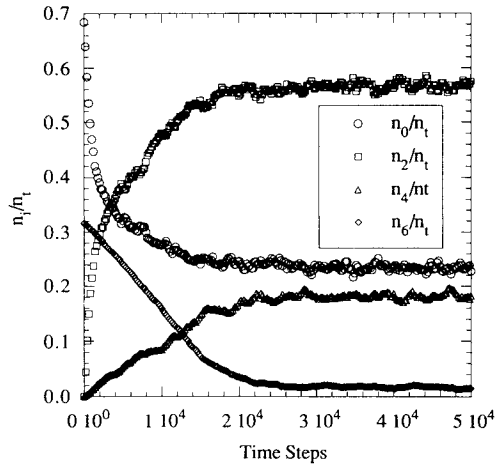


Fig. 8 Fractional populations in individual rotational states during relaxation of case III of Fig. 5. Initial population fractions: $n_0/n_1 = 0.684$, $n_2/n_1 = 0$, $n_4/n_1 = 0$, and $n_6/n_1 = 0.316$.

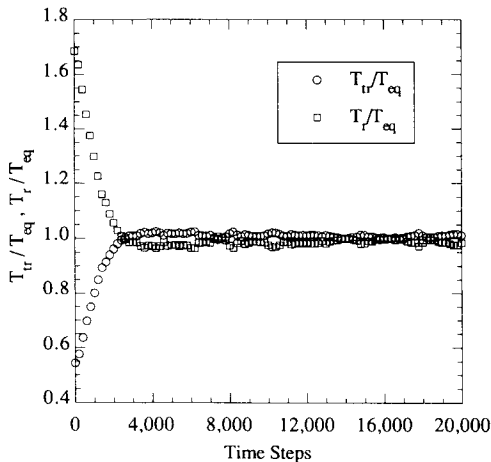


Fig. 9 Translational and rotational temperatures during relaxation of case I of Fig. 5.

libration of the states 0, 2, and 4, and the much slower excitation of state 6.

Case III illustrates this effect more dramatically. The state-to-state simulation predicts a significant increase in rotational temperature prior to the decrease to the final equilibrium value. Two separate simulations were carried out and are shown in the figure as an indication of the reproducibility of the results. The initial increase of rotational energy and tem-

perature arises from rapid population transfer from state 0 to state 2, followed by the much slower relaxation from state 6. This behavior cannot be simulated by the rotational relaxation models implemented in most current DSMC codes. Although the initial rotational distribution for these cases is artificial, similar types of distributions might arise in a gas where highly excited rotational levels are populated selectively by radiation or chemical reactions.

Computational Requirements

The simulations were run on a CRAY Y-MP. The B-L model required approximately $8.3 \mu\text{s}$ per time step per simulated particle, and the state-to-state model required approximately $24 \mu\text{s}$ per time step per particle. The time required for either model scales directly with the number of particles. The additional time required by the state-to-state model arises from the need to calculate a collision cross section each time a collision pair is chosen. Additionally, the β -factor used to obtain better statistics for processes with small cross sections increases the number of collision samples and, therefore, the computational time. Neither code is vectorized at present and we expect considerably enhanced speeds after vectorization.

Conclusions

The results of the simulation of rotational relaxation with state-to-state cross sections indicate that simple relaxation models, such as the Borgnakke-Larsen model, fail to reproduce the actual relaxation behavior. In certain cases it may be possible to adjust the theoretical rotational collision number to reproduce the relaxation of the mean rotational energy with acceptable accuracy. However, the reduction required may be difficult to predict a priori. If the initial state has strong nonequilibrium with highly excited states selectively populated by radiation or chemical reactions, then the simple models will fail to reproduce the relaxation behavior even qualitatively.

It does not appear to be practical to apply the state-to-state simulation to the analysis of complex flows, particularly of gases with more closely spaced rotational levels. Studies of homogeneous relaxation problems of the type described in this article should provide the basis for improvement of the simple models that must be used in these cases. An approach similar to the one described by Hermina¹⁸ may also be possible if representative states are to be tracked in a DSMC computation.

Acknowledgments

This work was supported by the Texas Advanced Research Program. Computing resources were provided by the University of Texas System Center for High Performance Computing. The authors gratefully acknowledge the assistance of Iain Boyd who provided a version of his DSMC code that was the starting point of our work.

References

- ¹Bird, G. A., *Molecular Gas Dynamics*, Oxford Univ. Press, London, 1976.
- ²Capitelli, M., Gorse, C., and Billing, G. D., "V-V Pumping Up in Non-Equilibrium Nitrogen: Effects on the Dissociation Rate," *Chemical Physics*, Vol. 52, No. 3, 1980, pp. 299-304.
- ³Jaffe, R. L., "The Calculation of High-Temperature Equilibrium and Nonequilibrium Specific Heat Data for N_2 , O_2 and NO ," AIAA Paper 87-1633, Honolulu, HI, June 1987.
- ⁴Bird, G. A., "Monte-Carlo Simulation in an Engineering Context, Rarefied Gas Dynamics," *Technical Papers from the 12th International Symposium*, Vol. 74, Pt. 1, Progress in Astronautics and Aeronautics, AIAA, New York, 1980, p. 252.
- ⁵Borgnakke, C., and Larsen, P., "Statistical Collision Model for Monte Carlo Simulation of Polyatomic Gas Mixtures," *Journal of Computational Physics*, Vol. 18, No. 4, 1975, p. 405.
- ⁶Parker, J. G., "Rotational and Vibrational Relaxation in Diatomic Gases," *Physics of Fluids*, Vol. 2, No. 4, 1959, pp. 449-462.

⁷Lordi, J. A., and Mates, R. E., "Rotational Relaxation in Nipolar Diatomic Gases," *Physics of Fluids*, Vol. 13, No. 2, 1970, pp. 291-308.

⁸Lumpkin, F. E., III, Chapman, D. R., and Park, C., "A New Rotational Relaxation Model for Use in Hypersonic Computational Fluid Mechanics," AIAA Paper 89-1737, Buffalo, NY, June 1989.

⁹Boyd, I. D., "Rotational-Translational Energy Transfer in Rarefied Nonequilibrium Flows," *Physics of Fluids A*, Vol. 2, No. 3, 1990, p. 447.

¹⁰Rabitz, H., and Lam, S.-H., "Rotational Energy Relaxation in Molecular Hydrogen," *Journal of Chemical Physics*, Vol. 63, No. 8, 1975, p. 3532.

¹¹Zarur, G., and Rabitz, H., "Effective Potential Formulation of Molecule-Molecule Collisions with Application to H_2-H_2 ," *Journal of Chemical Physics*, Vol. 60, No. 5, 1974, p. 2057.

¹²Green, S., "Rotational Excitation in H_2-H_2 Collisions: Close-Coupling Calculations," *Journal of Chemical Physics*, Vol. 62, No. 6, 1975, p. 2271.

¹³Monchick, L., and Schaefer, J., "Theoretical Studies of H_2-H_2

Collisions. II. Scattering and Transport Cross-Sections of Hydrogen at Low Energies: Tests of a New Ab-Initio Vibrotor Potential," *Journal of Chemical Physics*, Vol. 73, No. 12, 1980, p. 6153.

¹⁴Bird, G. A., "Perceptions of Numerical Methods in Rarefied Gasdynamics," *Rarefied Gas Dynamics: Theoretical and Computational Techniques*, Vol. 118, Progress in Astronautics and Aeronautics, AIAA, New York, 1989, p. 211.

¹⁵Baganoff, D., and McDonald, J. D., "A Collision-Selection Rule for a Particle Simulation Method Suited to Vector Computers," *Physics of Fluids A*, Vol. 2, No. 7, 1990, pp. 1248-1259.

¹⁶Radzig, A. A., and Smirnov, B. M., "Reference Data on Atoms, Molecules, and Ions," *Springer Series in Chemical Physics*, Vol. 31, Springer-Verlag, Berlin, 1985, p. 340.

¹⁷Lambert, J. D., *Vibrational and Rotational Relaxation in Gases*, Clarendon Press, Oxford, England, UK, 1977, Chap. 5, Tables 5.1 and 5.4, p. 120.

¹⁸Hermima, W. L., "Monte Carlo Simulation of High Altitude Rocket Plumes with Nonequilibrium Molecular Energy Exchange," AIAA Paper 86-1318, Boston, MA, June 1986.

Progress in Astronautics and Aeronautics

Gun Muzzle Blast and Flash

Günter Klingenberg and Joseph M. Heimerl

The book presents, for the first time, a comprehensive and up-to-date treatment of gun muzzle blast and flash. It describes the gas dynamics involved, modern propulsion systems, flow development, chemical kinetics and reaction networks of flash suppression additives as well as historical work. In addition, the text presents data to support a revolutionary viewpoint of secondary flash ignition and suppression.

The book is written for practitioners and novices in the flash suppression field: engineers, scientists, researchers, ballisticians, propellant designers, and those involved in signature detection or suppression.

1992, 551 pp, illus, Hardback, ISBN 1-56347-012-8,
AIAA Members \$65.95, Nonmembers \$92.95
Order #V-139 (830)

Place your order today! Call 1-800/682-AIAA



American Institute of Aeronautics and Astronautics
Publications Customer Service, 9 Jay Gould Ct., P.O. Box 753, Waldorf, MD 20604
Phone 301/645-5643, Dept. 415, FAX 301/843-0159

Sales Tax: CA residents, 8.25%; DC, 6%. For shipping and handling add \$4.75 for 1-4 books (call for rates for higher quantities). Orders under \$50.00 must be prepaid. Please allow 4 weeks for delivery. Prices are subject to change without notice. Returns will be accepted within 15 days.